Spatial variability of HV5 hardness in industrial direct chill cast EN AW-5083 ingots in the as-cast and homogenized conditions

Natalija Dolić, Zdenka Zovko Brodarac, Franjo Kozina

University of Zagreb, Faculty of Metallurgy, Sisak, Croatia

E-mail: ndolic@simet.unizg.hr, zovko@simet.unizg.hr, fkozin@simet.unizg.hr

(Received 27 March 2026; Accepted 07 June 2026)

Abstract

This study examines the spatial variability of HV5 hardness in industrially produced Direct Chill (DC) cast EN AW-5083 aluminium alloy ingots in the as-cast and homogenized conditions. Hardness measurements were performed at predefined sampling positions in the front and rear sections of six ingots using a Latin square design and evaluated by analysis of variance (ANOVA), coefficients of variation, correlation analysis, and linear regression. The results indicate a uniform longitudinal hardness distribution, with similar mean HV5 values at the front and rear sections, while significantly larger variations occur across the ingot cross-section. Slice height (*i*) and slice width (*j*) were identified as the dominant sources of variability. Homogenization reduced the overall mean HV5 from 81.8 HV5 to 75.7 HV5, decreased the coefficient of variation from 5.56% to 4.64%, and increased the correlation coefficient from r = 0.76 to r = 0.85. A statistically significant but limited relationship between the number of grains per unit area (N_A) and hardness was observed, indicating that N_A contributes to local hardness variations but is not the dominant factor controlling the overall spatial hardness distribution. The results indicate that homogenization does not increase hardness but improves its spatial homogeneity primarily through reduction of local microstructural and compositional heterogeneity.

Keywords: *EN AW-5083; Direct Chill casting; homogenization; Vickers hardness; spatial variability; statistical analysis*

1. Introduction

Aluminium-magnesium (Al-Mg) alloys of the 5xxx series are widely used in structural applications requiring low density, good weldability, corrosion resistance, and formability [1-4]. Among these, EN AW-5083 is recognised as one of the highest-strength non-heat-treatable aluminium alloys and is extensively used in marine structures, transportation systems, and pressure equipment [3, 4]. Its mechanical performance and corrosion behavior are governed primarily by Mg content and overall chemical composition [5, 6].

In EN AW-5083, strengthening is achieved predominantly through solid-solution strengthening due to Mg enrichment of the α-Al matrix [5].

Grain structure, represented in this study by the number of grains per unit area (N_A), may influence local hardness, as grain refinement generally increases resistance to plastic deformation [7, 8]. However, in DC-cast Al–Mg ingots, hardness variability may also be influenced by segregation-related compositional heterogeneity, local solute redistribution, and spatial variations in interdendritic microstructural constituents formed during solidification and homogenization [9-13]. Alloying elements and thermo-mechanical processing influence recrystallization and final grain size in magnesium-rich aluminium alloys [14].

Industrial production of large EN AW-5083 semi-finished products is typically carried out by the semi-continuous DC casting process, which leads to spatially non-uniform solidification conditions within the ingot cross-section [15, 16]. During DC casting, shell formation at the mould wall and intensive secondary cooling produce thermal gradients and different local cooling rates between the surface and the ingot centre [16-18]. These variations influence dendritic growth, grain formation, and chemical homogeneity [19, 20]. At the same time, thermosolutal convection, solidification shrinkage, and solute transport within the mushy zone promote macrosegregation, whose intensity increases with ingot size and sump depth [10, 17, 21, 22].

Previous investigations on industrial EN AW-5083 ingots have demonstrated spatial variations in hardness, mechanical properties, and grain structure caused by non-uniform solidification conditions during DC casting [23-26]. Statistical approaches, including analysis of variance (ANOVA), have been successfully applied to evaluate structural homogeneity and identify dominant sources of variability in such ingots [24-27]. However, previous studies have generally analysed grain structure or mechanical properties separately [23-27], while the direct statistical relationship between grain structure quantified by the number of grains per unit area (N_A) and hardness distribution at identical sampling positions has been addressed only to a limited extent. In addition, although hardness measurements in the as-cast condition have been reported previously [23], a comprehensive analysis combining spatial hardness distribution in both as-cast and homogenized conditions with statistical evaluation and correlation with grain structure at identical sampling positions has not been systematically investigated.

Homogenization heat treatment of DC-cast 5xxx alloys is primarily intended to reduce microsegregation and chemical gradients formed during non-equilibrium solidification [11, 12]. During homogenization, diffusion processes redistribute alloying elements and modify the morphology and distribution of interdendritic phases, thereby reducing local microstructural and compositional heterogeneity, while macrosegregation established during casting remains largely unaffected [10, 11, 13, 28].

The novelty of this study lies in the combined statistical and microstructural evaluation of spatial hardness variability in industrial DC-cast EN AW-5083 ingots at identical sampling locations in both as-cast and homogenized conditions. Unlike previous studies, which primarily considered grain structure or hardness separately, this work integrates Latin square statistical analysis with direct correlation between hardness (HV5) and previously quantified grain structure parameters (N_A) at corresponding sampling positions. This approach enables evaluation of the relationship between spatial hardness variability and local variations in grain structure within large industrial ingots.

Therefore, the aim of this study was to evaluate the spatial distribution and variability of HV5 hardness in industrial DC-cast EN AW-5083 ingots in the as-cast and homogenized conditions, and to analyse its relationship with previously quantified grain structure parameters (N_A). Given that EN AW-5083 is a non-heat-treatable alloy predominantly strengthened by solid-solution mechanisms [5], homogenization is not expected to significantly increase the mean HV5 value. It is therefore hypothesised that homogenization reduces the spatial variability of hardness within industrial EN AW-5083 ingots primarily through reduction of local microstructural and compositional heterogeneity, without increasing the mean hardness.

2. Experimental

The investigations were conducted on EN AW-5083 aluminium alloy ingots produced under full industrial conditions by a semi-continuous Direct Chill (DC) casting process using Pechiney technology. Six casting charges (3112, 3113, 3114, 3116, 3117, and 3120) were examined. The ingots had nominal dimensions of 520 mm × 1680 mm × 5100 mm. Their

chemical compositions complied with EN 573-3 [29] and corresponded to previously published data for the same industrial production route [23]. The melts were prepared from primary aluminium (commercial-purity A5 aluminium ingots) and technological scrap, followed by standard industrial treatments including refining, alloying, grain refinement, degassing, and filtration before casting.

Sampling was performed on cross-sectional slices approximately 30 mm thick, taken from the front (F) and rear (R) parts of each ingot after removal of technological scrap. In this study, front and rear sections refer to longitudinal positions along the ingot axis. In the as-cast condition, samples were taken from the lower half of each slice, while samples intended for homogenization were taken from mirror-symmetrical positions in the upper half, thereby ensuring comparable solidification and cooling conditions.

Sampling positions were selected according to a Latin square experimental design with six levels of slice height (*i*), corresponding to ingot thickness, and six levels of slice width (*j*), corresponding to ingot width, resulting in 36 predefined sampling positions in each longitudinal section. Each charge appeared once in each row and column of the experimental matrix (Figure 1).

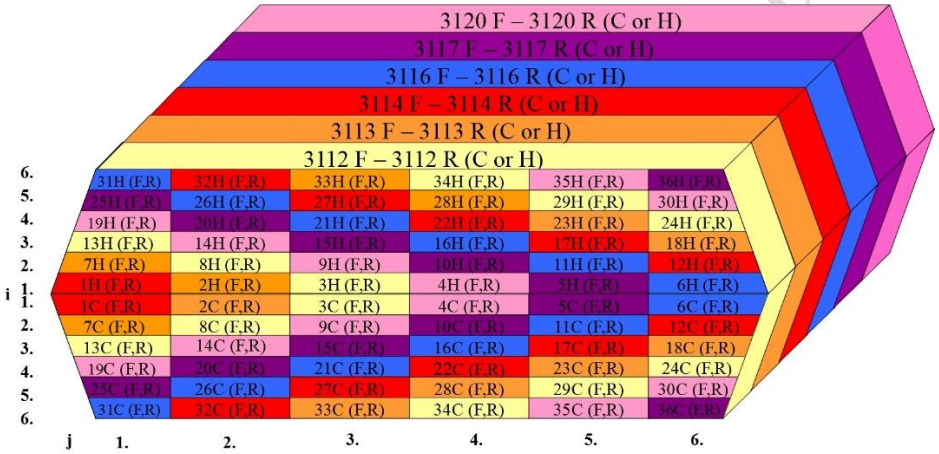

Figure 1. *Sampling scheme of EN AW-5083 ingot slices according to the Latin square experimental design; (i) denotes slice height (ingot thickness) and (j) denotes slice width (ingot width) [25, 27]*

Homogenization heat treatment was conducted under semi-industrial conditions in an AVS250 Durferrit salt bath at 520 °C for 10 h, followed by water quenching [23, 27]. As EN AW-5083 is a non-heat-treatable Al-Mg alloy, the treatment was applied to reduce chemical and microstructural heterogeneity generated during solidification, rather than to induce precipitation hardening.

Vickers hardness measurements (HV5) were performed at predefined sampling positions in both the as-cast and homogenized conditions, with 36 positions analysed per longitudinal section. Test specimens measuring approximately 30 × 30 mm and 5 mm thick were prepared from the selected locations. Hardness was measured using a Mitutoyo HV 112–114 hardness testing machine in accordance with EN ISO 6507-1 [30]. For positions near the slice edges (short edge, long edge, and top positions), six indentations were made from the edge towards the interior, while five indentations were made at all other positions. The arithmetic mean was taken as the representative hardness value for each sampling location and is hereafter referred to as the mean HV5. Additional statistical evaluation of hardness variability was performed using standard deviation and coefficient of variation analyses based on grouped HV5 data for charge, slice height, and slice width variables. To avoid overstating experimental precision, mean HV5 values are reported to one decimal place where appropriate. Particular attention was

given to edge regions because local solidification conditions and microstructural heterogeneity can significantly affect hardness [15, 21, 25]. Therefore, positions located 1–2 mm from the slice edges, corresponding to $i = 6$ and $j = 1$ and $j = 6$, were included in the analysis.

Statistical evaluation of hardness results was conducted using analysis of variance (ANOVA) based on a Latin square model. The effects of charge (six levels), slice height (i), and slice width (j) were assessed using the F-test, and the corresponding F-statistics and p-values were calculated. Statistical significance was determined at $\alpha = 0.05$. Calculations were performed using StatSoft® STATISTICA 13.2 and R (version 4.4.3).

Predefined sampling positions within each ingot slice were used to ensure consistent spatial evaluation of hardness distribution across the ingot cross-section. The Latin square design was applied to achieve balanced statistical evaluation of variability associated with slice height and width positions, while hardness measurements were performed independently at each predefined sampling location. Before ANOVA evaluation, residual diagnostics were examined to assess the assumptions of normality and homogeneity of variance.

To quantify the spatial homogeneity of hardness, the coefficient of variation (V) of mean HV5 values was calculated for all measurement positions within each slice. Mean HV5 values were also determined separately for the front (F) and rear (R) sections of the ingots. For each slice, the coefficient of variation was calculated as the ratio of the standard deviation to the mean HV5 value and expressed as a percentage. The arithmetic mean of these values is hereafter referred to as the mean coefficient of variation. The notations V_C and V_H were used to denote the coefficients of variation in the as-cast condition (C) and homogenized condition (H), respectively. The effect of homogenization was evaluated by comparing mean HV5 values and coefficients of variation in the as-cast and homogenized conditions.

The relationship between HV5 values measured at the front (F) and rear (R) sections was evaluated using Pearson's correlation coefficient based on paired HV5 measurements at identical sampling positions (n = 36). Correlation coefficients were determined separately for the as-cast and homogenized conditions and are denoted as $r_{c,CF–CR}$ and $r_{c,HF–HR}$, respectively. Additionally, the total correlation coefficient $r_{c,total}$ was calculated from pooled data, while charge-wise coefficients were determined for each casting charge (n = 6). Linear regression analysis was also conducted to quantify the relationship between front and rear HV5 values.

The grain structure at the same predefined sampling locations was previously characterized using the Latin square scheme, with the grain structure quantified by the number of grains per unit area (N_A) in the as-cast and homogenized conditions [23]. As the previously published structural characterization was expressed as the number of grains per unit area (N_A), the same parameter has been retained in the present statistical evaluation. In this work, the published N_A values were paired with the corresponding HV5 values at identical sampling locations to analyse the relationship between grain structure and hardness; therefore, the dataset is not presented here. The association between HV5 and N_A was evaluated using Pearson's correlation coefficient and simple linear regression ($HV5 = a + b \cdot N_A$). The analysis was performed separately for the front and rear sections in both conditions (n = 36 per dataset), with each dataset consisting of paired HV5 and N_A values obtained at identical sampling positions. The analysis was intended to evaluate the statistical correlation between N_A and hardness distribution rather than to establish a direct Hall–Petch-type relationship.

3. Results

3.1. Spatial Distribution of HV5 Hardness in the As-Cast and Homogenized EN AW-5083 Ingots

Tables 1 and 2 present the mean HV5 values measured at the predefined sampling locations (Figure 1) in the front and rear sections of the EN AW-5083 ingots in both the as-cast and

homogenized conditions. In the as-cast condition, the HV5 values in the front sections of the ingots ranged from 74.0 to 95.9, while those in the rear sections ranged from 75.3 to 90.8. After homogenization, the HV5 values ranged from 70.9 to 83.6 in the front sections and from 70.4 to 84.9 in the rear sections.

Table 1. *Hardness (HV5) values for the as-cast samples from the front and rear sections of the tested EN AW-5083 ingots (data adapted from [23])*

Sample Number	Mean HV5	Sample Number	Mean HV5	Sample Number	Mean HV5	Sample Number	Mean HV5
1FC-short	83.5	19FC-short	85.6	1RC-short	86.7	19RC-short	83.7
2FC	77.3	20FC	78.3	2RC	76.6	20RC	80.8
3FC	79.6	21FC	80.0	3RC	75.3	21RC	77.9
4FC	79.9	22FC	76.7	4RC	78.5	22RC	76.5
5FC	74.0	23FC	79.7	5RC	76.8	23RC	75.8
6FC-short	81.2	24FC-short	89.8	6RC-short	84.3	24RC-short	86.9
7FC-short	85.1	25FC-short	83.3	7RC-short	83.5	25RC-short	85.0
8FC	78.7	26FC	80.2	8RC	79.4	26RC	82.6
9FC	76.4	27FC	79.8	9RC	77.4	27RC	80.6
10FC	77.1	28FC	77.9	10RC	79.7	28RC	81.4
11FC	78.7	29FC	80.0	11RC	80.4	29RC	80.4
12FC-short	87.5	30FC-short	87.2	12RC-short	89.8	30RC-short	83.2
13FC-short	95.9	31FC-top	91.3	13RC-short	90.0	31RC-top	88.4
14FC	78.6	32FC-long	87.7	14RC	79.2	32RC-long	81.9
15FC	76.9	33FC-long	86.3	15RC	78.6	33RC-long	85.9
16FC	78.7	34FC-long	89.9	16RC	78.8	34RC-long	82.5
17FC	79.4	35FC-long	83.2	17RC	76.3	35RC-long	80.8
18FC-short	81.8	36FC-top	83.0	18RC-short	84.9	36RC-top	90.8

FC – front of ingot (as-cast condition); RC – rear of ingot (as-cast condition); short – short edge position; long – long edge position; top – top position in slice

Table 2. *Hardness (HV5) values for the homogenized samples from the front and rear sections of the tested EN AW-5083 alloy ingots*

Sample Number	Mean HV5	Sample Number	Mean HV5	Sample Number	Mean HV5	Sample Number	Mean HV5
1FH-short	76.9	19FH-short	80.3	1RH-short	78.3	19RH-short	79.5
2FH	72.1	20FH	74.8	2RH	73.6	20RH	75.4
3FH	71.2	21FH	73.4	3RH	70.9	21RH	74.8
4FH	71.8	22FH	72.8	4RH	70.4	22RH	72.4
5FH	72.8	23FH	74.5	5RH	73.4	23RH	72.5
6FH-short	77.4	24FH-short	75.7	6RH-short	80.1	24RH-short	76.1
7FH-short	77.3	25FH-short	78.6	7RH-short	78.6	25RH-short	78.7
8FH	70.9	26FH	74.6	8RH	73.6	26RH	76.8
9FH	73.1	27FH	73.0	9RH	73.2	27RH	72.5
10FH	72.0	28FH	74.1	10RH	72.5	28RH	72.3
11FH	72.2	29FH	72.9	11RH	74.0	29RH	73.2
12FH-short	80.2	30FH-short	83.6	12RH-short	77.2	30RH-short	79.6
13FH-short	80.8	31FH-top	81.9	13RH-short	80.3	31RH-top	84.9
14FH	74.6	32FH-long	81.2	14RH	75.3	32RH-long	76.8
15FH	72.6	33FH-long	78.3	15RH	73.2	33RH-long	77.2
16FH	72.3	34FH-long	77.2	16RH	74.9	34RH-long	77.0
17FH	71.5	35FH-long	79.3	17RH	72.7	35RH-long	76.4
18FH-short	76.9	36FH-top	80.2	18RH-short	80.2	36RH-top	78.6

FH – front of ingot (homogenized condition); RH – rear of ingot (homogenized condition); short – short edge position; long – long edge position; top – top position in slice

The mean HV5 values measured at the front and rear longitudinal sections were very similar in both conditions (Table 3). In the as-cast condition, the mean values were 82.0 HV5 at the front and 81.7 HV5 at the rear [20], while after homogenization they decreased to 75.6 and 75.8 HV5, respectively. When averaged over both sections, the overall mean HV5 decreased from 81.8 HV5 in the as-cast condition to 75.7 HV5 after homogenization, corresponding to a reduction of 7.5%. Homogenization also improved the spatial homogeneity of hardness, as indicated by the lower mean coefficient of variation.

Table 3. *Mean HV5 values and mean coefficients of variation for the front and rear sections of the ingots in the as-cast [23] and homogenized conditions*

Section	Mean HV5	Mean V/%
FC	82.0	5.70
RC	81.7	5.42
C	81.8	5.56
FH	75.6	4.88
RH	75.8	4.40
H	75.7	4.64

3.2. Influence of Charge and Cross-Sectional Position on Hardness (Latin Square and ANOVA Analysis)

Tables 4 and 5 summarise the mean HV5 values, parameter estimates, standard deviations, and coefficients of variation for the front and rear sections in the as-cast and homogenized conditions. Measurable variability in HV5 values was observed within the investigated sampling groups. The largest deviations from the overall mean HV5 are associated with slice height (*i*) and slice width (*j*) in both conditions.

Table 4. *Mean HV5 values, parameter estimates, standard deviations, and coefficients of variation (V_C) for the front and rear sections of the ingots in the as-cast condition*

Variables	Level	Mean HV5 (C)		Parameter Estimate		Standard deviation		V_C/%	
		F	R	F	R	F	R	F	R
Charge	3112	85.7	82.4	3.70	0.71	7.17	5.32	8.37	6.45
	3113	81.4	81.4	-0.60	-0.35	3.74	4.27	4.59	5.25
	3114	82.4	82.0	0.48	0.26	4.55	5.43	5.52	6.63
	3116	81.7	82.1	-0.27	0.36	4.81	3.90	5.89	4.76
	3117	78.8	82.0	-3.18	0.25	3.68	5.13	4.67	6.26
	3120	81.8	80.5	-0.13	-1.24	4.21	2.57	5.14	3.19
Slice height (*i*)	1.	79.3	79.7	-2.70	-2.00	3.28	4.67	4.14	5.86
	2.	80.6	81.7	-1.37	0.00	4.58	4.43	5.69	5.43
	3.	81.9	81.3	-0.07	-0.40	7.05	5.13	8.61	6.31
	4.	81.7	80.3	-0.27	-1.44	4.99	4.38	6.10	5.45
	5.	81.4	82.2	-0.55	0.50	3.33	1.76	4.09	2.14
	6.	86.9	85.1	4.95	3.35	3.41	3.99	3.93	4.69
Slice width (*j*)	1.	87.5	86.2	5.50	4.51	5.06	2.63	5.79	3.05
	2.	80.1	80.1	-1.82	-1.62	3.82	2.17	4.77	2.71
	3.	79.8	79.3	-2.12	-2.42	3.53	3.67	4.42	4.63
	4.	80.0	79.6	-1.92	-2.14	4.97	2.15	6.21	2.70
	5.	79.2	78.4	-2.78	-3.29	2.97	2.34	3.76	2.99
	6.	85.1	86.7	3.13	4.95	3.54	3.09	4.16	3.56

Table 5. *Mean HV5 values, parameter estimates, standard deviations, and coefficients of variation (V_H) for the front and rear sections of the ingots in the homogenized condition*

Variables	Level	Mean HV5 (H)	Parameter Estimate	Standard deviation	V_H/%

		F	R	F	R	F	R	F	R
Charge	3112	74.8	75.2	-0.86	-0.57	3.86	3.32	5.16	4.42
	3113	75.5	75.7	-0.11	-0.02	2.35	3.38	3.11	4.46
	3114	75.9	75.0	0.29	-0.77	4.12	2.73	5.43	3.64
	3116	75.3	77.6	-0.34	1.83	3.76	4.20	4.99	5.42
	3117	75.2	75.3	-0.47	-0.45	3.45	2.77	4.59	3.68
	3120	77.1	75.7	1.48	-0.02	4.64	3.60	6.02	4.75
Slice height (*i*)	1.	73.7	74.5	-1.94	-1.30	2.73	3.94	3.70	5.29
	2.	74.3	74.9	-1.36	-0.90	3.65	2.45	4.91	3.28
	3.	74.8	76.1	-0.86	0.35	3.53	3.36	4.72	4.42
	4.	75.3	75.1	-0.39	-0.64	2.68	2.63	3.56	3.50
	5.	76.1	75.5	0.50	-0.24	4.21	3.26	5.53	4.32
	6.	79.7	78.5	4.04	2.73	1.77	3.23	2.22	4.12
Slice width (*j*)	1.	79.3	80.1	3.66	4.30	2.01	2.48	2.54	3.10
	2.	74.7	75.3	-0.94	-0.50	3.56	1.43	4.77	1.91
	3.	73.6	73.6	-2.04	-2.12	2.43	2.15	3.30	2.93
	4.	73.4	73.3	-2.27	-2.50	2.05	2.33	2.79	3.18
	5.	73.9	73.7	-1.77	-2.05	2.84	1.43	3.85	1.93
	6.	79.0	78.6	3.36	2.88	2.90	1.67	3.66	2.13

3.2.1. Influence of Individual Variables on Hardness in the As-Cast Condition

Figure 2 shows the influence of charge, slice height, and slice width on the mean HV5 values in the as-cast condition for the front and rear sections. The mean HV5 values at the two longitudinal positions remain similar in both sections.

A systematic increase in hardness towards the slice edges is observed in both longitudinal sections. At the ingot front, the highest positive parameter estimates for slice width occur at j = 1 and j = 6, reaching +5.50 and +3.13 HV5, respectively, while at the rear they reach +4.51 and +4.95 HV5 (Table 4). Similarly, the highest mean HV5 values with respect to slice height occur at the outer level i = 6, amounting to 86.9 HV5 at the front and 85.1 HV5 at the rear.

The ANOVA results for the as-cast condition are presented in Table 6. Slice height and slice width are statistically significant sources of variability in both longitudinal sections. Slice height is significant at the front (p = 0.002) and rear (p = 0.010), whereas slice width is highly significant at both positions (p < 0.001). Charge is statistically significant only in the front section (p = 0.010).

The coefficients of variation indicate moderate dispersion of hardness values within the as-cast ingots. They range from 3.76% to 8.61% at the front and from 2.14% to 6.63% at the rear, with mean values of 5.70% and 5.42%, respectively (Tables 3 and 4).

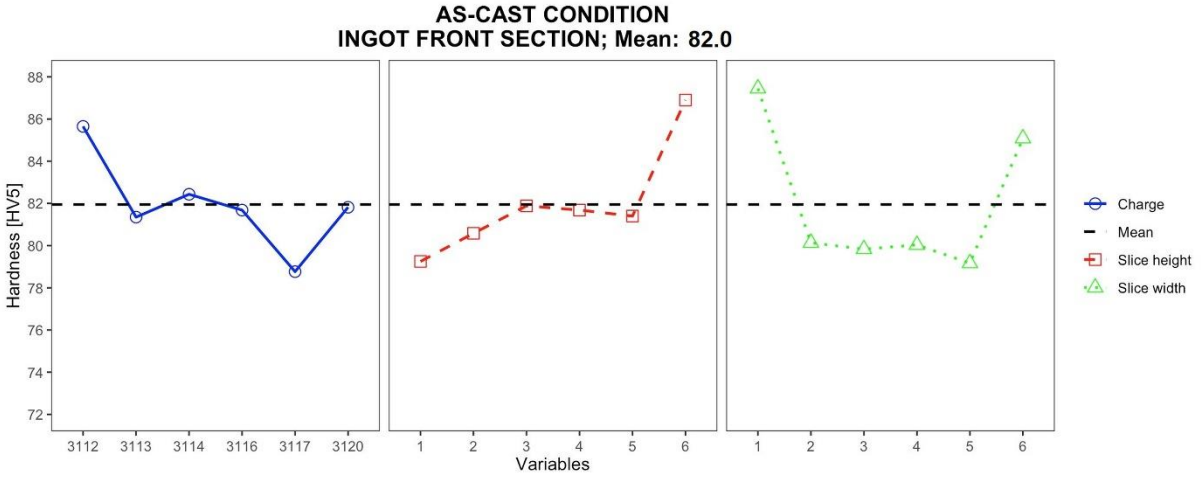

(a)

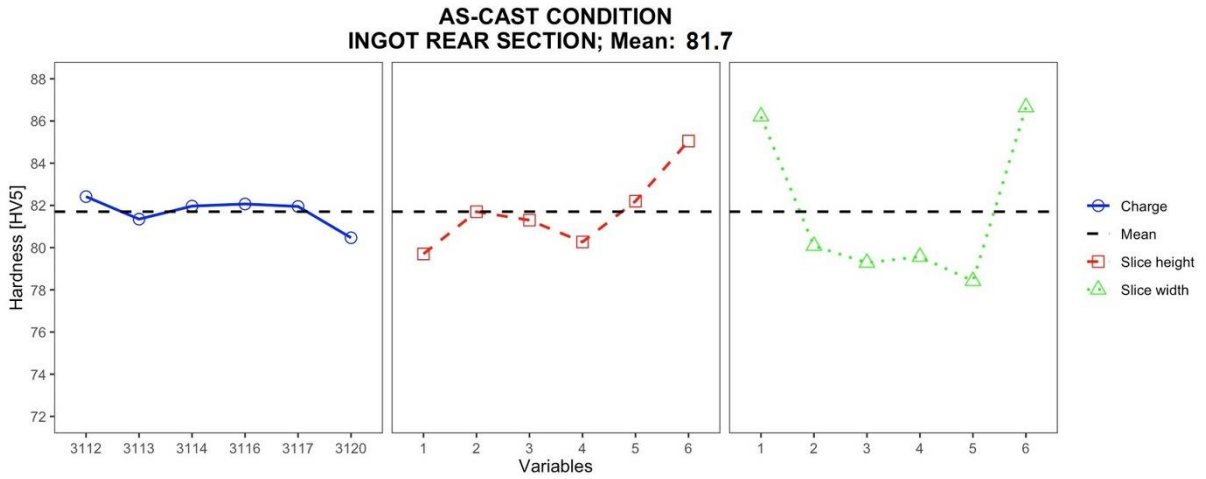

(b)

Figure 2. *Effect of individual variables on mean HV5 hardness in the as-cast condition: (a) ingot front section; (b) ingot rear section*

Table 6. *ANOVA results for HV5 hardness in the ingot front and rear sections in the as-cast condition*

Variable	SS		df		MS		F		p	
	F	R	F	R	F	R	F	R	F	R
Charge	147.04	14.55	5	5	29.41	2.91	4.13	0.57	0.010	0.726
Slice height (*i*)	204.23	106.12	5	5	40.85	21.22	5.73	4.12	0.002	0.010
Slice width (*j*)	355.61	412.13	5	5	71.12	82.43	9.98	16.01	<0.001	<0.001
Residual	142.47	102.97	20	20	7.12	5.15				

SS, sum of squares; df, degrees of freedom; MS, mean square

3.2.2. Influence of Individual Variables on Hardness in the Homogenized Condition

Figure 3 shows the influence of charge, slice height, and slice width on the mean HV5 values in the homogenized condition. The positional trends are similar to those observed in the as-cast condition, but the overall mean HV5 values are lower in both longitudinal sections (Table 3).

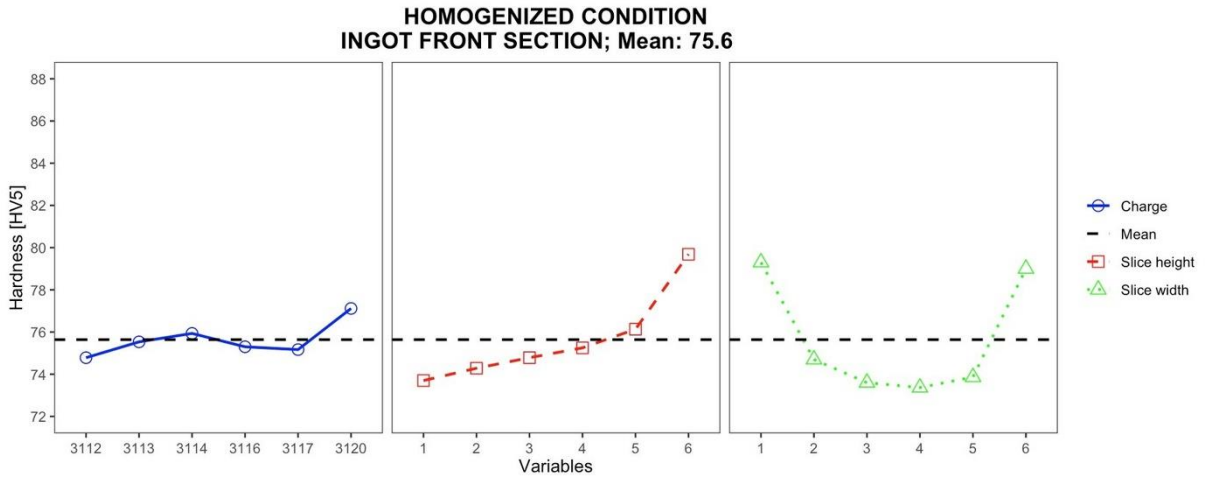

(a)

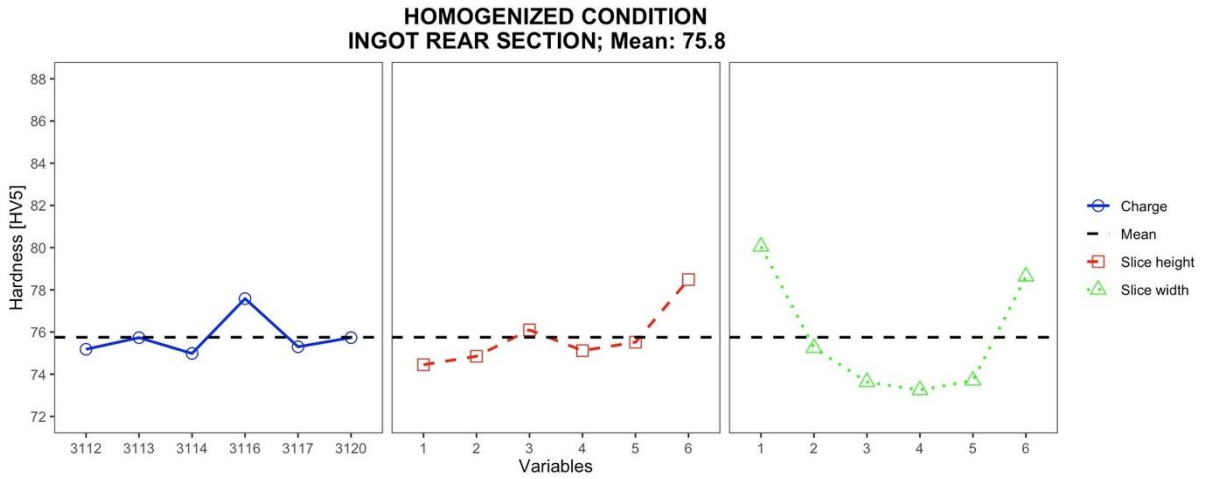

(b)

Figure 3. *Effect of individual variables on mean HV5 hardness in the homogenized condition: (a) ingot front section; (b) ingot rear section*

The effect of charge is less pronounced after homogenization, whereas slice height and slice width remain the dominant sources of variability. For slice height, the estimated deviations from the overall mean HV5 at the ingot front range from −1.94 HV5 at $i = 1$ to +4.04 HV5 at $i = 6$, with a similar trend at the rear (Table 5). Higher HV5 values are observed at $j = 1$ and $j = 6$.

The ANOVA results for the homogenized condition are presented in Table 7. Slice height and slice width are statistically significant in both longitudinal sections ($p < 0.001$). Charge is not statistically significant at the front ($p = 0.271$), but remains significant at the rear ($p = 0.009$).

The coefficients of variation are lower than in the as-cast condition, ranging from 2.22% to 6.02% at the front and from 1.91% to 5.42% at the rear. The mean coefficient of variation decreases from 5.56% in the as-cast condition to 4.64% after homogenization (Tables 3 and 5).

Table 7. *ANOVA results for HV5 hardness in the ingot front and rear sections (homogenized condition)*

Variable	SS		df		MS		F		p	
	F	R	F	R	F	R	F	R	F	R
Charge	20.11	26.84	5	5	4.02	5.37	1.39	4.21	0.271	0.009
Slice height (*i*)	138.50	63.29	5	5	27.70	12.66	9.56	9.93	<0.001	<0.001
Slice width (*j*)	228.26	251.92	5	5	45.65	50.38	15.76	39.52	<0.001	<0.001
Residual	57.93	25.50	20	20	2.90	1.28				

3.3. Correlation between HV5 Values Measured at the Front and Rear Sections of the Ingots

Table 8 presents the correlation between HV5 values measured at identical positions in the front and rear sections. A strong positive relationship is observed in both conditions, indicating consistent front–rear hardness behavior. The total correlation coefficient increases from $r_{c,CF–CR} = 0.76$ in the as-cast condition to $r_{c,HF–HR} = 0.85$ after homogenization. The very high correlation coefficients observed for some individual charges are likely influenced by the limited number of paired observations per charge (n = 6).

Table 8. *Pearson correlation coefficients between the front and rear HV5 values for each casting charge in the as-cast ($r_{c,CF–CR}$) and homogenized ($r_{c,HF–HR}$) conditions, together with the total correlation coefficient ($r_{c,total}$)*

Charge	3112	3113	3114	3116	3117	3120	$r_{c,total}$
$r_{c,CF–CR}$	0.90	0.76	0.78	0.86	0.91	0.96	0.76
$r_{c,HF–HR}$	0.96	0.78	0.85	0.99	0.98	0.94	0.85

3.4. Relationship between the Number of Grains per Unit Area (N_A) and Hardness (HV5)

Previously published number of grains per unit area values for identical sampling positions [20] were paired with the corresponding HV5 values to evaluate the relationship between grain structure and hardness. Linear regression analysis was performed using 36 paired N_A and mean HV5 values for each ingot section.

In the as-cast condition, statistically significant positive N_A–HV5 relationships were observed for both longitudinal sections (Figure 4). For the front section, the regression equation is HV5 = 71.96 + 0.155·N_A (R^2 = 0.274, r = 0.523, p = 0.001), while for the rear section it is HV5 = 78.17 + 0.055·N_A (R^2 = 0.114, r = 0.337, p = 0.044). Thus, higher N_A values are generally associated with slightly higher HV5 values.

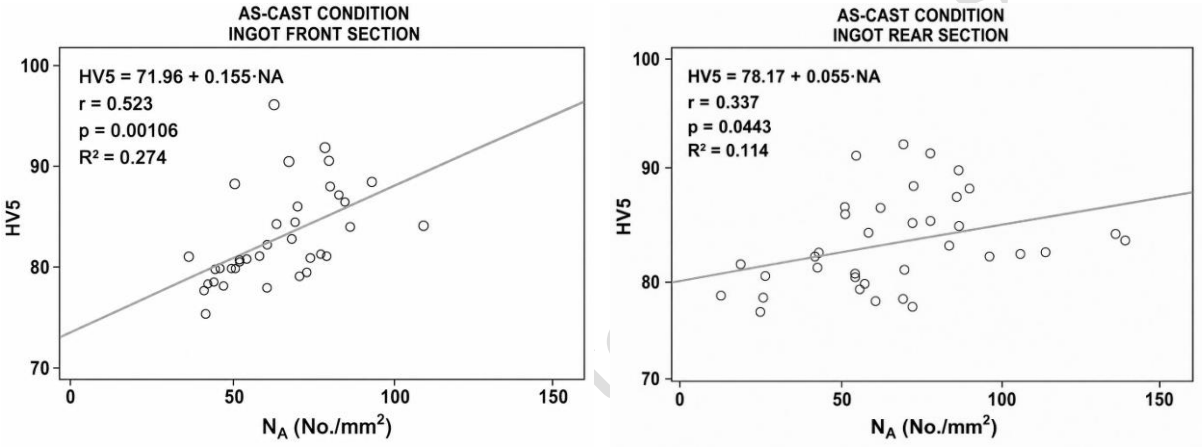

(a) (b)

Figure 4. *Correlation between number of grains per unit area (N_A) and mean HV5 hardness in the as-cast condition: (a) ingot front section; (b) ingot rear section*

After homogenization, the N_A–HV5 relationship remains statistically significant in both sections (Figure 5). For the front section, the regression equation is HV5 = 67.25 + 0.110·N_A (R^2 = 0.339, r = 0.582, $p < 0.001$), while for the rear section it is HV5 = 72.14 + 0.048·N_A (R^2 = 0.154, r = 0.392, p = 0.018).

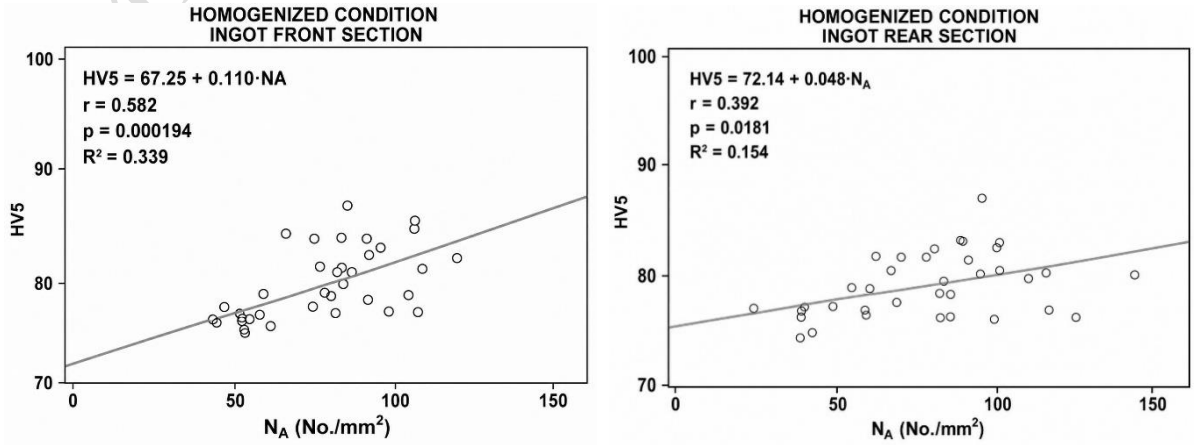

(a) (b)

Figure 5. *Correlation between number of grains per unit area (N_A) and mean HV5 hardness in the homogenized condition: (a) ingot front section; (b) ingot rear section*

For direct comparison, the regression parameters are summarized in Table 9. The relatively low coefficients of determination (R^2 = 0.114–0.339) indicate limited to moderate statistical association between N_A and HV5. Overall, homogenization is associated with lower mean HV5 values, reduced variability, and preservation of positive N_A–HV5 trends.

Table 9. *Summary of linear regression parameters describing the relationship between number of grains per unit area (N_A) and mean HV5 hardness in the as-cast and homogenized conditions*

Condition	Section	Regression equation (HV5)	Pearson r	R^2	p
As-cast	Front	$HV5 = 71.96 + 0.155 \cdot N_A$	0.523	0.274	0.001
As-cast	Rear	$HV5 = 78.17 + 0.055 \cdot N_A$	0.337	0.114	0.044
Homogenized	Front	$HV5 = 67.25 + 0.110 \cdot N_A$	0.582	0.339	<0.001
Homogenized	Rear	$HV5 = 72.14 + 0.048 \cdot N_A$	0.392	0.154	0.018

4. Discussion

The results indicate that hardness in the investigated EN AW-5083 ingots is relatively uniform along the longitudinal direction, whereas significantly larger variations occur across the ingot cross-section. The mean HV5 values measured at the front and rear sections in the as-cast condition are very similar (82.0 HV5 and 81.7 HV5), while the positive correlation coefficient $r_{c,CF–CR}$ = 0.76 confirms a consistent front–rear hardness pattern along the casting direction (Tables 3 and 8). After homogenization, the corresponding mean values remain similar (75.6 HV5 and 75.8 HV5), and the correlation increases to $r_{c,HF–HR}$ = 0.85 (Tables 3 and 8). This indicates that longitudinal variations are limited in both conditions and that hardness heterogeneity is mainly associated with the ingot cross-section. This is further supported by the reduction in the coefficient of variation after homogenization, indicating improved spatial homogeneity of hardness (Table 3).

Statistical analysis confirms that hardness variability is governed by spatial factors within the cross-section. The ANOVA results and parameter estimates (Tables 4–7, Figures 2 and 3) identify slice height (*i*) and slice width (*j*) as the dominant sources of variability in both conditions. In the as-cast condition, slice height is statistically significant at both longitudinal positions (p = 0.002 and p = 0.010), while slice width exhibits the strongest effect ($p < 0.001$) (Table 6), and this trend persists after homogenization (Table 7). This behavior is characteristic of DC casting, where thermal gradients and solidification conditions vary across the ingot cross-section [10, 15]. Cooling rate variations contribute to spatial differences in microstructural development and hardness response [31, 32]. Such behavior may also be associated with local variations in secondary dendrite arm spacing (SDAS), which is inversely related to cooling rate and may contribute to spatial differences in microstructural morphology, segregation behavior, and hardness response in cast aluminium alloys [33]. In addition to grain structure effects, spatial hardness variations in DC-cast EN AW-5083 ingots may also be influenced by segregation-related compositional heterogeneity formed during non-equilibrium solidification. The spatial hardness distribution supports this interpretation. In the as-cast condition, the highest HV5 values occur predominantly in edge regions, particularly at positions corresponding to j = 1 and j = 6 and i = 6, as shown in Table 1 and reflected by the parameter estimates in Table 4 and Figure 2. The maximum value (95.9 HV5) was recorded at an edge position, indicating that local solidification conditions near the ingot surface, associated with higher cooling rates, may contribute to local microstructural heterogeneity and corresponding differences in hardness response compared with the ingot interior [15, 34].

Local hardness differences may also be influenced by the spatial distribution of Mg-containing phases such as Mg_2Si, which form in interdendritic regions and contribute to local microstructural heterogeneity and spatial variations in mechanical response in DC-cast AA5xxx alloys [12, 13]. Previous microstructural analysis of charge 3116 showed a reduction in the surface fraction of Mg_2Si after homogenization, consistent with its partial dissolution into the matrix, while Fe- and Mn-based intermetallic phases remained relatively stable [24].

The relationship between the number of grains per unit area (N_A) and hardness is positive but limited. The N_A–HV5 correlations (Figures 4 and 5, Table 9) show that positions with higher N_A values tend to exhibit slightly higher hardness values, indicating a limited statistical association between grain-structure-related spatial variation and local hardness response, which is qualitatively consistent with previously reported grain structure–property trends [7, 8]. However, the relatively low coefficients of determination ($R^2 = 0.114–0.339$) indicate that N_A accounts for only a limited fraction of the total hardness variability. Therefore, the observed N_A–HV5 relationship should be interpreted as a statistical association between grain-density-related heterogeneity and hardness rather than as direct evidence of a Hall–Petch-type strengthening mechanism.

A direct comparison of sampling location, N_A, and hardness (HV5) shows that variations across the ingot cross-section (*i* and *j* directions) are more pronounced than those between the front and rear sections. Although a positive relationship between N_A and HV5 is observed, similar positional trends in hardness occur regardless of local variations in N_A. This indicates that N_A alone cannot adequately describe the spatial hardness distribution.

The observed decrease in mean hardness, reduction in variability, and increase in longitudinal correlation after homogenization indicate that the primary effect of homogenization is the reduction of local microstructural and compositional heterogeneity within the ingot.

5. Conclusions

The results show that hardness in industrial DC-cast EN AW-5083 ingots is relatively uniform along the casting direction, while significantly larger variations occur across the ingot cross-section, governed primarily by slice height (*i*) and slice width (*j*). In the as-cast condition, the higher HV5 values observed in edge regions reflect locally intensified cooling conditions and associated microstructural and compositional heterogeneity. Homogenization reduces the mean HV5 from 81.8 to 75.7 and improves spatial homogeneity, as confirmed by a reduction in the coefficient of variation and an increase in longitudinal correlation between the front and rear sections. The relationship between the number of grains per unit area (N_A) and hardness is positive but limited, indicating that N_A contributes to local variations but cannot be considered a reliable predictor of the overall hardness distribution. The relatively low coefficients of determination further indicate that hardness variability is controlled by multiple interacting factors. Overall, homogenization improves the spatial homogeneity of hardness within the ingot. The results obtained may contribute to improved process evaluation and optimization during industrial production and homogenization of large DC-cast EN AW-5083 ingots.

Acknowledgements

The investigation was carried out as part of the Institutional Research Project the "Design and characterisation of innovative engineering alloys/products (KIIL)" financed by the EU – Next Generation EU. The views and opinions expressed are those of the author and do not necessarily reflect the official positions of the European Union or the European Commission. Neither the European Union nor the European Commission can be held responsible for them. The investigation was performed on equipment within the infrastructural scientific projects:

*Center for Founding - SIMET (Code: KK.01.1.1.02.0020); and the VIRTULAB - Integrated Laboratory for Primary and Secondary Raw Materials (Code: KK.01.1.1.02.0022) and HQCastScrap - Frontiers of using scrap raw materials for high quality castings (*24864*) funded by European Institute for Technology KIC Raw Materials.*

Author contributions

N. Dolić: Conceptualization, Methodology, Investigation, Formal analysis, Writing – original draft; Z. Zovko Brodarac: Writing – Review & Editing; F. Kozina: Writing – Review & Editing.

Data Availability

Data will be made available on request.

Conflicts of Interest

The authors declare no conflict of interest.

References

[1] D. Istrate, B.-G. Sbârcea, A.M. Demian, A.D. Buzatu, L. Salcianu, I. Bordeasu, L.M. Micu, C. Ghera, B. Florea, B. Ghiban, Correlation between mechanical properties—structural characteristics and cavitation resistance of cast aluminum alloy type 5083, Crystals, 12 (11) (2022) 1538. https://doi.org/10.3390/cryst12111538

[2] S. Toros, F. Ozturk, I. Kacar, Review of warm forming of aluminum–magnesium alloys, Journal of Materials Processing Technology, 207 (1–3) (2008) 1-12. https://doi.org/10.1016/j.jmatprotec.2008.03.057

[3] M.B.A. Ramadan, I. Esen, H. Ahlatci, E. Duran, Homogenization heat treatment for enhancing corrosion resistance and tribological properties of the Al5083-H111 alloy, Materials, 17 (13) (2024) 3313. https://doi.org/10.3390/ma17133313

[4] T. Tokarski, Thermo-mechanical processing of rapidly solidified 5083 aluminium alloy—structure and mechanical properties, Archives of Metallurgy and Materials, 60 (1) (2015) 177-180. https://doi.org/10.1515/amm-2015-0028

[5] C.-R. Song, B.-X. Dong, S.-Y. Zhang, H.-Y. Yang, L. Liu, J. Kang, J. Meng, C.-J. Luo, C.-G. Wang, K. Cao, J. Qiao, S.-L. Shu, M. Zhu, F. Qiu, Q.-C. Jiang, Recent progress of Al–Mg alloys: forming and preparation process, microstructure manipulation and application, Journal of Materials Research and Technology, 31 (2024) 3255-3286. https://doi.org/10.1016/j.jmrt.2024.07.051

[6] W. Zhou, F. Xue, M. Li, Corrosion behavior of Al–Mg alloys with different alloying element contents in 3.5% NaCl solution, Metals, 15 (3) (2025) 327. https://doi.org/10.3390/met15030327

[7] N. Hansen, Hall–Petch relation and boundary strengthening, Scripta Materialia, 51 (2004) 801–806. https://doi.org/10.1016/j.scriptamat.2004.06.002

[8] G. Jeong, J. Park, S. Nam, S.-E. Shin, J. Shin, D. Bae, H. Choi, The effect of grain size on the mechanical properties of aluminum, Archives of Metallurgy and Materials, 60 (2B) (2015) 1287-1291. https://doi.org/10.1515/amm-2015-0115

[9] A. Ćitić, T. Radetić, F. Rajković, D. Prelević, M. Popović, Evolution of microstructure under different homogenization conditions and its effect on recrystallization processes during hot rolling of AA5182 alloy, Journal of Mining and Metallurgy, Section B: Metallurgy, 61 (3) (2025) 369-383. https://doi.org/10.2298/JMMB250817029C

[10] R. Nadella, D.G. Eskin, Q. Du, L. Katgerman, Macrosegregation in Direct-Chill Casting of Aluminium Alloys, Progress in Materials Science, 53 (2008) 421-480. https://doi.org/10.1016/j.pmatsci.2007.10.001

[11] O. Engler, K. Kuhnke, J. Hasenclever, Development of intermetallic particles during solidification and homogenization of two AA 5xxx series Al–Mg alloys with different Mg contents, Journal of Alloys and Compounds, 728 (2017) 669-681. https://doi.org/10.1016/j.jallcom.2017.09.060
[12] T. Radetić, M. Popović, E. Romhanji, Microstructure evolution of a modified AA5083 aluminum alloy during a multistage homogenization treatment, Materials Characterization, 65 (2012) 16-27. https://doi.org/10.1016/j.matchar.2011.12.006
[13] O. Engler, S. Miller-Jupp, Control of second-phase particles in the Al–Mg–Mn alloy AA 5083, Journal of Alloys and Compounds, 689 (2016) 998-1010. https://doi.org/10.1016/j.jallcom.2016.08.070
[14] V. Aryshenskii, F. Grechnikov, E. Aryshenskii, Y. Erisov, S. Konovalov, M. Tepterev, A. Kuzin, Alloying elements effect on the recrystallization process in magnesium-rich aluminum alloy, Materials, 15 (20) (2022) 7062. https://doi.org/10.3390/ma15207062
[15] D.G. Eskin, Physical Metallurgy of Direct Chill Casting of Aluminum Alloys, CRC Press, Boca Raton, 2008.
[16] H. Zhao, Z. Zhang, Y. Bai, B. Li, M. Gao, Numerical and experimental study on the direct chill casting of large-scale AA2219 billets via annular coupled electromagnetic field, Materials, 15 (5) (2022) 1802. https://doi.org/10.3390/ma15051802
[17] A. Pakanati, M. M'Hamdi, H. Combeau, M. Založnik, Investigation of macrosegregation formation in aluminium DC casting for different alloy systems, Metallurgical and Materials Transactions A, 49 (10) (2018) 4710-4721. https://doi.org/10.1007/s11661-018-4731-z
[18] Y.-X. Zhang, J.-S. Wang, D.-X. Chen, B. Wang, C. Zhang, Z.-A. Wang, Effects of cooling rates on microporosity in DC casting Al–Li alloy, China Foundry, 19 (2) (2022) 177-190. https://doi.org/10.1007/s41230-022-1183-2
[19] N. Jamaly, N. Haghdadi, A.B. Phillion, Microstructure, macrosegregation, and thermal analysis of direct chill cast AA5182 aluminum alloy, Journal of Materials Engineering and Performance, 24 (5) (2015) 2067–2073. https://doi.org/10.1007/s11665-015-1480-7
[20] Q. Han, Dendritic features of the solidification structure in a large AA3004 direct chill (DC) cast ingot, Metallurgical and Materials Transactions B, 53B (2022) 786-797. https://doi.org/10.1007/s11663-022-02423-7
[21] D.G. Eskin, Mechanisms and control of macrosegregation in DC casting, in Light Metals 2014 (J. Grandfield, Ed.), John Wiley & Sons, Hoboken, 2014, p. 855-860. https://doi.org/10.1002/9781118888438.ch143
[22] D.G. Eskin, R. Nadella, L. Katgerman, Effect of different grain structures on centerline macrosegregation during direct-chill casting, Acta Materialia, 56 (6) (2008) 1358-1365. https://doi.org/10.1016/j.actamat.2007.11.021
[23] N. Dolić, Z. Zovko Brodarac, F. Kozina, Hardness Testing of Al–Mg Slabs, Proc. 6th Metallurgical & Materials Engineering Congress of South-East Europe, June 4–7, 2025, Trebinje, Bosnia and Herzegovina, p. 7-13.
[24] N. Dolić, Utjecaj uvjeta skrućivanja i hlađenja na svojstva polukontinuirano lijevanih blokova Al–Mg slitine (Influence of Solidification and Cooling Conditions on the Properties of Semicontinuous Cast Slabs of Al–Mg Alloy). PhD Thesis, University of Zagreb, Faculty of Metallurgy, Sisak, Croatia, 2010. (*in Croatian*)
[25] N. Dolić, Z. Zovko Brodarac, Evaluation of EN AW-5083 aluminum alloy homogeneity using statistical analysis of mechanical properties, Journal of Mining and Metallurgy, Section B: Metallurgy, 53 (3) (2017) 429-439. https://doi.org/10.2298/JMMB170812046D
[26] N. Dolić, A. Markotić, F. Unkić, Structural Homogeneity of Direct-Chill Cast Ingots of Aluminum Alloy EN AW-5083, Metallurgical and Materials Transactions B, 38 (2007) 491–495. https://doi.org/10.1007/s11663-006-9008-z

[27] N. Dolić, Z. Zovko Brodarac, S. Manasijević, Influence of Homogenization on Structural Homogeneity of Aluminum Alloy EN AW-5083, Proc. 46th International October Conference on Mining and Metallurgy, October 1–4, 2014, Bor, Serbia, p. 597-600.
[28] D. Istrate, C. Lazar, O.P. Odagiu, A.M. Demian, A.D. Buzatu, B. Ghiban, Influence of homogenization and aging parameters applied to mechanical and structural characteristics of alloy 5083, IOP Conference Series: Materials Science and Engineering, 1262 (2022) 012021. https://doi.org/10.1088/1757-899X/1262/1/012021
[29] European Committee for Standardization, EN 573-3:2009 Aluminium and aluminium alloys—chemical composition and form of wrought products—Part 3: Chemical composition and form of products, CEN, Brussels, 2009.
[30] International Organization for Standardization, ISO 6507-1:2023 Metallic Materials—Vickers Hardness Test—Part 1: Test Method, ISO, Geneva, 2023.
[31] A. Rahman, S.P. Isanaka, F. Liou, A Comprehensive Study of Cooling Rate Effects on Diffusion, Microstructural Evolution, and Characterization of Aluminum Alloys, Machines, 13 (2025) 160. https://doi.org/10.3390/machines13020160
[32] G.L. Faria, A.S. Leite, The Effect of Casting Speed and the Fraction of Al5%Ti1%B Inoculant on the Microstructure and Mechanical Properties of the AA5052 Aluminum Alloy Produced by the Direct Chill Process, Materials Research, 21 (2) (2018**)** e20170872. https://doi.org/10.1590/1980-5373-mr-2017-0997
[33] I. Sari, M. Ahmadein, S. Ataya, L. Hachani, K. Zaidat, N. Alrasheedi, M. Wu, A. Kharicha, Prediction of the secondary dendrite arm spacing based on dendrite tip kinetics and cooling rate, Materials, 17 (4) (2024) 865. https://doi.org/10.3390/ma17040865
[34] J. Wang, Y. Zuo, Q. Zhu, B. Li, M. Gao, Numerical simulation of melt flow and temperature field during DC casting 2024 aluminium alloy under different casting conditions, China Foundry, 21 (2024) 387–396. https://doi.org/10.1007/s41230-024-3099-5

LIST OF FIGURE CAPTIONS

LIST OF TABLE CAPTIONS